ChemPubSoc Europe

DOI: 10.1002/ejic.201501381

EurJIC European Journal of Inorganic Chemistry

Full Paper

Ruthenium Catalysts

Synthesis, Structural Characterization, and Catalytic Activity of Indenyl Tris(*N*-pyrrolyl)phosphine Complexes of Ruthenium

Matthew J. Stark,[a] Michael J. Shaw,[b] Nigam P. Rath,[a,c] and Eike B. Bauer*[a]

Abstract: The synthesis, characterization, and catalytic activity of new ruthenium complexes of the tris(*N*-pyrrolyl)phosphine ligand [P(pyr)$_3$] are described. The new ruthenium complexes [RuCl(ind)(PPh$_3$){P(pyr)$_3$}] and [RuCl(ind){P(pyr)$_3$}$_2$] (ind = indenyl, η^5-C$_9$H$_7^-$) were synthesized in 73 and 63 % isolated yields, respectively, by thermal ligand exchange of [RuCl(ind)(PPh$_3$)$_2$] with P(pyr)$_3$. The electronic and steric properties of the new complexes were studied through analysis of the X-ray structures and cyclic voltammetry. The new complexes [RuCl(ind)(PPh$_3$)-{P(pyr)$_3$}] and [RuCl(ind){P(pyr)$_3$}$_2$] and the known complex [RuCl(ind){(PPh$_3$)$_2$}] differed only slightly in their steric properties, as seen from the comparable bond lengths and angles around the ruthenium centers. The oxidation potentials of [RuCl(ind)(PPh$_3$){P(pyr)$_3$}] and [RuCl(ind){P(pyr)$_3$}$_2$] of +0.34 and +0.71 V versus Cp$_2$Fe$^{0/+}$ (Cp = cyclopentadienyl) are substantially higher than that of [RuCl(ind)(PPh$_3$)$_2$] (–0.023 V), in accordance with the enhanced π-acidity of the P(pyr)$_3$ ligand. The new complexes are catalytically active in the etherification of propargylic alcohols and in the first ruthenium-catalyzed formation of known and new xanthenones from propargylic alcohols and diketones (18 to 72 h at 90 °C in ClCH$_2$CH$_2$Cl or toluene, 1–2 mol-% catalyst, 69–22 % isolated yields).

Introduction

Transition-metal complexes of ruthenium are applied in broad fields such as catalysis[1] and optical devices.[2] In medicinal organometallic chemistry, ruthenium complexes are increasingly investigated as alternatives to platinum-based anticancer drugs (which are limited by side-effects).[1a,3,4] A plethora of ruthenium complexes are known, as are attempts to modify them to improve their performances in their respective applications. The electronic properties of ruthenium complexes are most commonly tuned through their ancillary ligands.[1c,4] Knowledge of the effects of ligands on the electronic (and steric) properties allows for the tailored synthesis of ruthenium complexes with unique properties for specialized applications.

Phosphines are probably still the most widely utilized ligand class in the synthesis and application of ruthenium complexes,[5] albeit other ligands such as carbenes[6] and imines[7] are increasingly utilized. Phosphine ligands bearing aryl and alkyl groups are the most common ones used in the syntheses of metal complexes, and their electronic modification is achieved through the variation of the aryl substituents or the nature of the alkyl groups.[8] Although the tuning options are powerful, they are somewhat limited at times, as they sometimes require lengthy syntheses, which hamper practical applications. Thus, the search for readily available phosphine ligands with unique electronic properties is ongoing.

Tris(*N*-pyrrolyl)phosphine [P(pyr)$_3$, pyr = *N*-pyrrolyl] is a readily accessible ligand with electronic properties different from those of the PPh$_3$ ligand.[9] Research in the past decade has shown that P(pyr)$_3$ exhibits increased π-acidity[10] with electronic properties similar to those of CO.[9] IR ν_{CO} stretching frequencies are utilized frequently to assess the electronic properties of a ligand, and the electron-withdrawing properties of P(pyr)$_3$ were demonstrated through the IR ν_{CO} stretching frequencies of its rhodium chlorido carbonyl complex.[9] Furthermore, the oxidation potential, as determined by cyclic voltammetry, indicates the π-acidity of P(pyr)$_3$.[11] Further electronic tuning is possible by placing electron-withdrawing substituents on the pyrrolyl ring.[12] A few ruthenium complexes of P(pyr)$_3$[13] and their catalytic applications are known (Figure 1).[11] Nevertheless, the chemistry of P(pyr)$_3$ complexes of ruthenium is far less explored than that of PPh$_3$ and its analogs. We think that improved knowledge of the coordination chemistry of this ligand will open the pathway for its use in the synthesis of tailored ruthenium complexes.

As part of our longstanding research program directed towards the catalytic activation of propargylic alcohols,[14,15] we were interested in investigating electron-poor ruthenium complexes. Propargylic alcohols can be catalytically activated by ruthenium complexes,[16] for example, through the formation of ruthenium allenylidene complexes [Ru=C=C=CR$_2$]$^{2+}$,[14,17] and we speculated that the reactivity of potential allenylidene intermediates with nucleophiles would increase with decreased electron density at the metal center. The known[18] ruthenium

[a] *Department of Chemistry and Biochemistry, University of Missouri – St. Louis, One University Boulevard, St. Louis, MO 63121, USA*
E-mail: bauere@umsl.edu
www.eike-bauer.net
[b] *Department of Chemistry, Southern Illinois University Edwardsville, Edwardsville, IL 62025, USA*
[c] *Center for Nanoscience, University of Missouri, St. Louis, MO, USA*

Supporting information and ORCID(s) from the author(s) for this article are available on the WWW under http://dx.doi.org/10.1002/ejic.201501381.

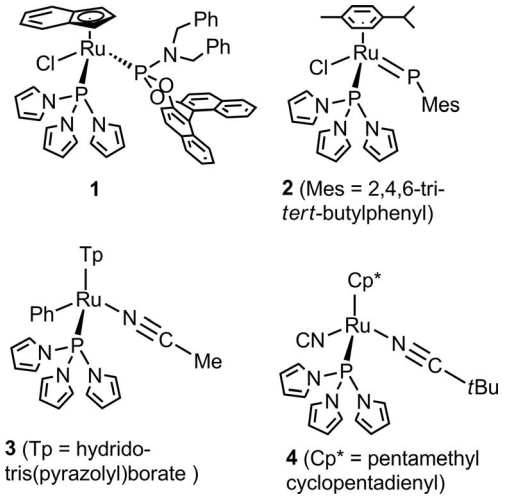

Figure 1. Representative $P(pyr)_3$ complexes of ruthenium.

indenyl complex $[RuCl(ind)(PPh_3)_2]$ (ind = η^5-$C_9H_7^-$) has been utilized previously as a starting material for organometallic syntheses,[19] and ruthenium indenyl complexes are frequently applied in catalysis.[20] The increased reactivity of indenyl complexes compared to the analogous cyclopentadienyl complexes has been ascribed to the so-called "indenyl effect".[21] The formation of open coordination sites of the corresponding complexes is facilitated through an η^5–η^3 ring slip. The effect has been ascribed to increased aromaticity of the benzo portion of the ligand through a ring slip[21e] or related to the lower M–C bond energies of η^5-indenyl complexes compared with those of η^5-cyclopentadienyl (Cp) complexes.[21b] We were interested in synthesizing $P(pyr)_3$ analogues of $[RuCl(ind)(PPh_3)_2]$ to access ruthenium complexes of increased Lewis acidity with improved catalytic activity for the transformation of propargylic alcohols.

Herein, we describe the synthesis and characterization of the ruthenium complexes $[RuCl(ind)(PPh_3)\{P(pyr)_3\}]$ and $[RuCl(ind)\{P(pyr)_3\}_2]$. We assess the electronic properties of the new complexes through analysis of their X-ray structures and cyclic voltammetry. Finally, we demonstrate that the new complexes are catalytically active in the etherification of propargylic alcohols and in the first ruthenium-catalyzed formation of xanthenones from propargylic alcohols and diketones.

Results and Discussion

Ligand and Ruthenium Complex Syntheses

Several syntheses of $P(pyr)_3$ have been described previously.[9,10f] We prepared the ligand through a slightly modified literature procedure,[9] which is provided in the Supporting Information. In general, it is important to work under moisture-free conditions and distill all starting materials immediately before use.

The precursor complex $[RuCl(ind)(PPh_3)_2]$ has been used as a starting material for the syntheses of ruthenium complex through ligand-substitution reactions by us[13,15e,15f] and others.[22] Accordingly, when $[RuCl(ind)(PPh_3)_2]$ was heated with 1.1 equiv. of $P(pyr)_3$ in tetrahydrofuran (THF) under reflux for 4 h, the mono(pyrrolylphosphine) complex $[RuCl(ind)(PPh_3)\{P(pyr)_3\}]$ was isolated in 73 % yield as a red solid after chromatographic workup (Scheme 1). In a second ligand-exchange reaction, $[RuCl(ind)(PPh_3)\{P(pyr)_3\}]$ was heated with another equivalent of $P(pyr)_3$ in THF under reflux for 5 h. The bis(pyrrolylphosphine) complex $[RuCl(ind)\{P(pyr)_3\}_2]$ was obtained in 63 % yield as an orange-yellow solid after column chromatography. Attempts to access $[RuCl(ind)\{P(pyr)_3\}_2]$ directly from $[RuCl(ind)(PPh_3)_2]$ in a double ligand-exchange reaction failed, as the obtained mixtures of the mono- and disubstituted complexes made workup difficult and lowered the yield.

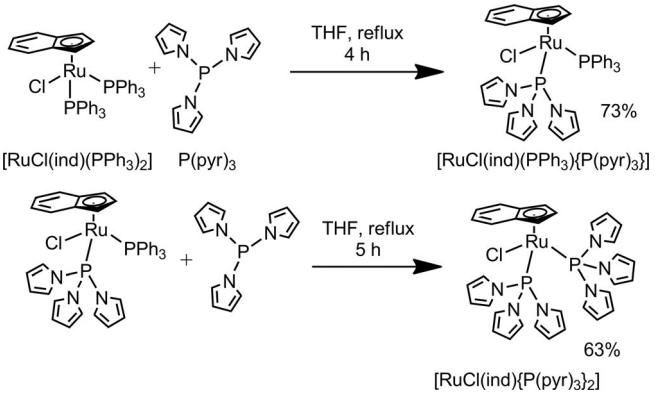

Scheme 1. Synthesis of $P(pyr)_3$ complexes of ruthenium.

The new complexes were characterized by multinuclear NMR spectroscopy, MS, IR spectroscopy, elemental analysis, and X-ray diffraction. In $[RuCl(ind)(PPh_3)\{P(pyr)_3\}]$, the coordination of one $P(pyr)_3$ ligand and one PPh_3 ligand is clearly indicated by two distinct $^{31}P\{^1H\}$ NMR signals at δ = 122.8 and 40.4 ppm, which exhibit a $^2J_{P,P}$ coupling constant of 144 Hz, as expected for complexes with two magnetically different phosphorus atoms in the metal coordination sphere. Free $P(pyr)_3$ resonates at δ = 78.8 ppm in the $^{31}P\{^1H\}$ NMR spectrum, and the chemical shifts for the complex indicate the coordination of the ligand. The complex $[RuCl(ind)\{P(pyr)_3\}_2]$ exhibited only one signal in its $^{31}P\{^1H\}$ NMR spectrum at δ = 122.2 ppm, as expected for two identical phosphorus atoms coordinated to the ruthenium center.

The indenyl ligand gives very distinct ^1H and $^{13}C\{^1H\}$ NMR signals for the three protons and the five carbon atoms of its coordinated five-membered ring.[23] Owing to the unsymmetrical substitution pattern with four different ligands in $[RuCl(ind)(PPh_3)\{P(pyr)_3\}]$, all of these carbons atoms and protons are diastereotopic and give individual signals in the corresponding NMR spectra. In $[RuCl(ind)\{P(pyr)_3\}_2]$, the complex is symmetric as has two $P(pyr)_3$ ligands, and the chemically equivalent protons and carbon atoms give only one set of signals for the cyclopentadienyl portion of the complex, which simplifies the ^1H and $^{13}C\{^1H\}$ NMR spectra.

X-ray Structures

To establish the structure of the new ruthenium complexes unequivocally, the X-ray structures of $[RuCl(ind)(PPh_3)\{P(pyr)_3\}]$ and $[RuCl(ind)\{P(pyr)_3\}_2]$ were determined (Table 1 and Figure 2). Se-

Table 1. Crystallographic parameters.

	[RuCl(ind)(PPh_3){P(pyr)$_3$}]	[RuCl(ind){P(pyr)$_3$}$_2$]	Xanthenone **7b**
Empirical formula	$C_{39}H_{34}ClN_3P_2Ru$	$C_{33}H_{31}ClN_6P_2Ru$	$C_{27}H_{24}O_3$
Formula weight	743.15	710.10	396.46
Temperature [K]/wavelength [Å]	100(2)/0.71073	100(2)/0.71073	100(2)/0.71073
Crystal system	orthorhombic	monoclinic	triclinic
Space group	*Pbca*	$P2_1/c$	$P\bar{1}$
a [Å]	17.9518(15)	13.2598(6)	10.1854(6)
b [Å]	15.6316(12)	9.5844(4)	12.5276(7)
c [Å]	24.057(2)	24.8271(11)	17.3162(9)
α [°]	90	90	105.980(3)
β [°]	90	99.205(2)	92.278(3)
γ [°]	90	90	107.377(3)
Volume [Å^3]/*Z*	6750.8(9)/8	3114.6(2)/4	2009.2(2)4
Density (calculated) [Mg/m^3]	1.462	1.514	1.311
Absorption coefficient [mm^{-1}]	0.672	0.726	0.084
F(000)	3040	1448	840
Crystal size [mm^3]	0.346 × 0.235 × 0.076	0.256 × 0.151 × 0.135	0.298 × 0.275 × 0.243
θ range for data collection [°]	1.924 to 27.161	1.556 to 36.325	1.234 to 30.571
Index ranges	$-21 \le h \le 23$	$-22 \le h \le 22$	$-12 \le h \le 14$
	$-20 \le k \le 15$	$-15 \le k \le 14$	$-17 \le k \le 17$
	$-30 \le l \le 27$	$-41 \le l \le 41$	$-24 \le l \le 24$
Reflections collected	78357	69845	48129
Independent reflections	7471 [*R*(int) = 0.0733]	15058 [*R*(int) = 0.0603]	12106 [*R*(int) = 0.0413]
Absorption correction	semiempirical from equivalents	semiempirical from equivalents	semiempirical from equivalents
Max. and min. transmission	0.7989 and 0.7989	0.8625 and 0.7561	0.8879 and 0.8189
Data/restraints/parameters	7471/1/415	15058/0/388	12106/1/541
Goodness-of-fit on F^2	1.003	1.019	1.028
Final *R* indices [$I > 2\sigma(I)$]	R_1 = 0.0319,	R_1 = 0.0361,	R_1 = 0.0525,
	wR_2 = 0.0604	wR_2 = 0.0745	wR_2 = 0.1314
R indices (all data)	R_1 = 0.0596,	R_1 = 0.0559,	R_1 = 0.0892,
	wR_2 = 0.0706	wR_2 = 0.0831	wR_2 = 0.1546
Largest diff. peak and hole [e/Å^3]	0.479 and −0.511	0.759 and −0.683	0.365 and −0.324

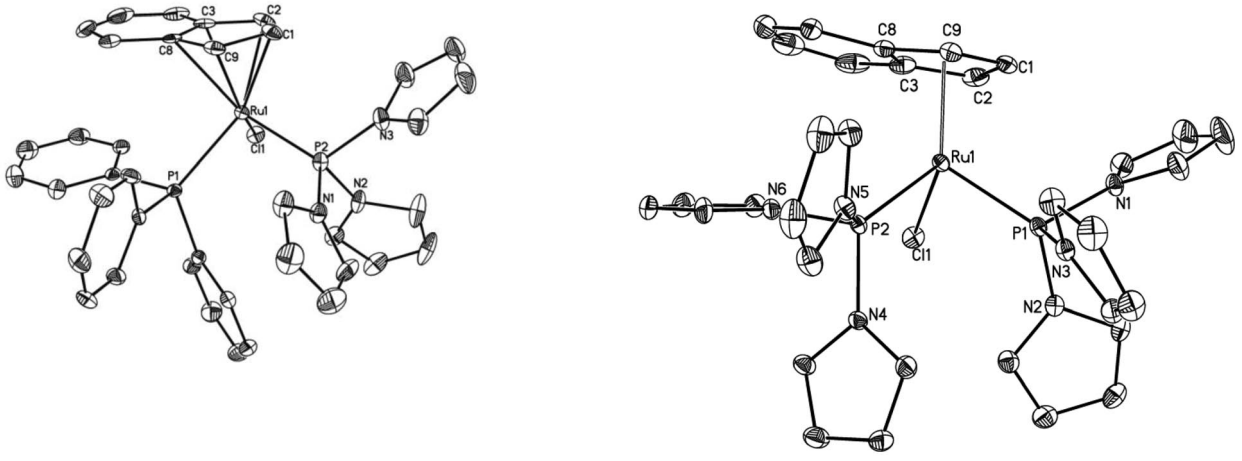

Figure 2. The molecular structures of [RuCl(ind)(PPh_3){P(pyr)$_3$}] (left) and [RuCl(ind){P(pyr)$_3$}$_2$] (right). Hydrogen atoms are omitted for clarity. The crystallographic parameters are compiled in Table 1, and key bond lengths and angles are listed in Table 2.

lected bond lengths and angles are listed in Table 2, and for comparison purposes, the X-ray data for [RuCl(ind)(PPh_3)$_2$] are also included.[24]

The bond angles for the monodentate ligands about the ruthenium center range from 89.510(13) to 99.008(14)°. Thus, the structures are best described as slightly distorted octahedra. For both complexes, the greatest deviation from the ideal 90° angle is for the P(1)–Ru–P(2) angle [97.89(5) and 99.008(14)°]; this suggests that some steric repulsion occurs between PPh_3 and P(pyr)$_3$ and between the two P(pyr)$_3$ ligands, respectively. Interestingly, the P(1)–Ru–P(2) angles for both complexes are comparable; therefore, the P(pyr)$_3$ and the PPh_3 ligands have similar steric demands.

The Ru–P bond length for the P(pyr)$_3$ ligand in [RuCl(ind)(PPh_3){P(pyr)$_3$}] [2.2323(15) Å] is only slightly shorter than that found for the PPh_3 ligand [2.2760(14) Å], which might

Table 2. Selected bond lengths [Å] and angles [°].

	[RuCl(Ind)(PPh_3){$P(pyr)_3$}]	[RuCl(Ind){$P(pyr)_3$}$_2$]	[RuCl(Ind)(PPh_3)$_2$]
Ru–P(1)	2.2323(15) [$P(Pyr)_3$]	2.2042(4)	2.331
Ru–P(2)	2.2760(14) (PPh_3)	2.2716(4)	2.268
Ru–Cl	2.4362(15)	2.4251(4)	2.437
P(1)–N(X)[a] average	1.712	1.716	–
P(1)–C(X)[a] average	1.831	–	–
P(1)–Ru–P(2)	97.89(5)	99.008(14)	99.21
Cl–Ru–P(1)	93.51(5)	90.684(14)	92.42
Cl–Ru–P(2)	91.79(5)	89.510(13)	92.19
Ru–Cp[b]	1.902	1.928	1.918
Δ Ru–C[c]	0.161	0.155	0.221
Fold angle[d]	7.06	7.33	7.07

[a] P(1)–N(X) corresponds to the P–N bonds of $P(pyr)_3$. P(1)–C(X) corresponds to the P–C bonds of PPh_3. [b] Distance between the Cp centroid of the indenyl ligand and the ruthenium center. [c] Average difference between the Ru–C1, Ru–C2, and Ru–C9 bond lengths and the Ru–C3 and Ru–C8 bond lengths, see Figure 3. [d] Angle between the planes formed by C1–C2–C9 and C2–C3–C8–C9, see Figure 3.

be due to increased backbonding from the ruthenium center to the $P(pyr)_3$ ligand.[11,13a] Furthermore, in [RuCl(ind){$P(pyr)_3$}$_2$], the Ru–P bond lengths of both $P(pyr)_3$ ligands are also slightly different [2.2042(4) and 2.2716(4) Å, respectively] but fall in the range found for other ruthenium $P(pyr)_3$ complexes.[11,14e] Also, the distances between the Cp centroids of the indenyl ligands and the ruthenium centers for both complexes are similar (1.902 and 1.928 Å) and comparable to that for [RuCl(ind)(PPh_3)$_2$] (1.918 Å). Thus, the angles and bond lengths for the $P(pyr)_3$ ligand are comparable to the those for PPh_3 ligand; overall, the geometric parameters for the two $P(pyr)_3$ complexes and [RuCl(ind)(PPh_3)$_2$] are similar, and the Ru–$P(pyr)_3$ bond lengths are at best slightly shorter than the Ru–$P(pyr)_3$ bond lengths.

The slightly longer P–N bond lengths of the $P(pyr)_3$ ligand (1.712 and 1.716 Å) than the typical P–N bond lengths of phosphoramidite ligands $R_2NP(OR)_2$ (ca. 1.66 Å) suggest a substantial P=N double-bond character in the phosphoramidite ligand.[13a,14a] The elongated P–N bond lengths in the $P(pyr)_3$ ligand are in accordance with the aromatic delocalization of the nitrogen lone pair into the five-membered pyrrolyl ring, as described previously,[9] and this delocalization prevents the formation of a double bond with the phosphorus atom.

As can be seen from the X-ray structures, the indenyl ligands for both complexes are η^5-coordinated, that is, all five carbon atoms of the cyclopentadienyl units form bonds to the ruthenium centers. However, as has been described previously, the Ru–C bonds in the coordinated cyclopentadienyl units are not all the same lengths in the two complexes described herein. As illustrated in Figure 3 (top left) with some exaggeration, the cyclopentadienyl units in indenyl complexes are typically slipped in a way that the bond lengths of the two benzenoid carbon atoms are longer than the bond lengths to the other three carbon atoms. This has been ascribed to a gain in resonance energy for the aryl ring of the ligand.[21e] In an extreme case, only three of the five carbon atoms would bond to the ruthenium center in an η^3 fashion (Figure 3, top right).[21e] The degree of the slippage has previously been quantified by two parameters taken from the X-ray data, the ΔM–C value and the fold angle.[21e,25] The ΔM–C value is the average difference between the Ru–C1, Ru–C2, and Ru–C9 bond lengths and the Ru–C3 and Ru–C8 bond lengths in the structures in Figure 2. Ideally, ΔM–C is 0, and values of ca. 0.2 Å are typical for indenyl ligands and indicate η^5-coordination. The values for [RuCl(ind)(PPh_3)-{$P(pyr)_3$}] and [RuCl(ind){$P(pyr)_3$}$_2$] fall in this range. The fold angle is the angle between the planes formed by C1–C2–C8 and C2–C3–C8–C9 (Figure 3, top right); it takes the value 0 in an ideal η^5 coordination, and the values are typically below 10° for indenyl complexes. Again, [RuCl(ind)(PPh_3){$P(pyr)_3$}] and [RuCl(ind){$P(pyr)_3$}$_2$] fall in this range. An η^3 coordination would be indicated by a fold angle of ca. 60°.[21e]

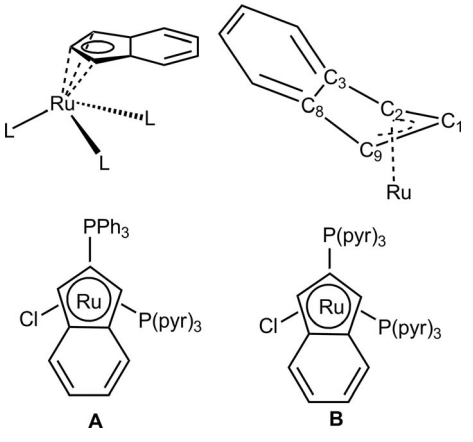

Figure 3. Geometric parameters for indenyl complexes.

However, what is interesting for the two complexes is which ligand takes the position *trans* to the C_3 and C_8 benzo carbon atoms of the cyclopentadienyl unit. It has been demonstrated before that the ligand with the strongest *trans* influence takes the positon *trans* to the benzo unit, and this weakens the bond strength (and enlarges the bond length) of the two Ru–C bonds of the benzo unit.[21e] In [RuCl(ind){$P(pyr)_3$}$_2$], one of the two $P(pyr)_3$ ligands is located *trans* to the benzo ring; therefore, $P(pyr)_3$ has a stronger *trans* influence than the chlorido ligand (**B** in Figure 3). However, in [RuCl(ind)(PPh_3){$P(pyr)_3$}], the PPh_3 ring is located in the *trans* position (**A** in Figure 3); therefore, PPh_3 has a stronger *trans* influence than $P(pyr)_3$. This observation might be ascribed to the higher σ-basicity of PPh_3 compared with that of $P(pyr)_3$, which leads to a stronger *trans* influence.

In the past, the basicity of ligands has been assessed through the ν_{CO} stretching frequencies of carbonyl complexes and, indeed, the higher value for $P(pyr)_3$ ($\tilde{\nu}$ = 2024 cm^{-1}) than that for PPh_3 ($\tilde{\nu}$ = 1980 cm^{-1}) in *trans*-[RhCl(CO)L_2] [L = $P(pyr)_3$, PPh_3] indicates the higher basicity of the latter.[9] Further evidence for the higher basicity of PPh_3 compared to $P(pyr)_3$ is provided by the ^{31}P–^{77}Se coupling constants, which increase with decreasing basicity of the phosphorus compound.[26] In accordance with the higher basicity of PPh_3, Se=$P(pyr)_3$ exhibits a $J_{P,Se}$ value of ca. 970 Hz, which is significantly higher than the corresponding value for Se=PPh_3 (735 Hz).[27]

Cyclic Voltammetry

Overall, the solid-state structures of [RuCl(ind)(PPh_3){$P(pyr)_3$}] and [RuCl(ind){$P(pyr)_3$}$_2$] revealed some similarities between these two complexes and [RuCl(ind)(PPh_3)$_2$]. The structural parameters around the ruthenium center are comparable and corroborate earlier statements that the PPh_3 and $P(pyr)_3$ ligands are sterically similar. Electronic differences could be observed through the stronger *trans* influence of PPh_3 compared with that of $P(pyr)_3$ and through the higher $J_{P,Se}$ coupling constants in Se=$P(pyr)_3$. Cyclic voltammetry has been used before to characterize the electronic properties of ruthenium phosphine complexes.[28] To obtain further insights into the electronic properties of the new complexes, we recorded the cyclic voltammograms of [RuCl(ind)(PPh_3){$P(pyr)_3$}] and [RuCl(ind){$P(pyr)_3$}$_2$] as well as that of [RuCl(ind)(PPh_3)$_2$] for comparison. The traces for a scan rate of 0.8 V/s are compiled in Figure 4.

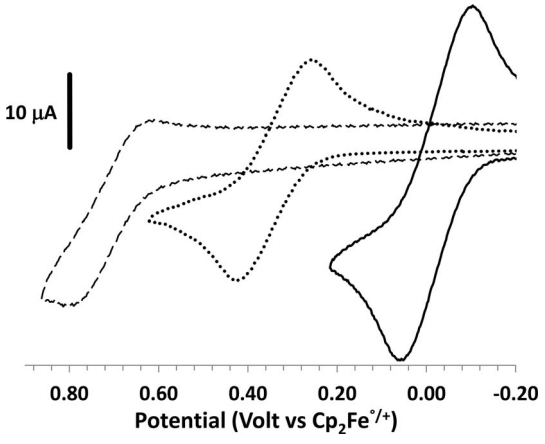

Figure 4. Cyclic voltammograms of ruthenium indenyl complexes in 0.1 M Bu_4PF_6/CH_2Cl_2 at 298 K and recorded at a scan rate of 0.8 V/s: [RuCl(ind)(PPh_3)$_2$] (solid line), [RuCl(ind)(PPh_3){$P(pyr)_3$}] (dotted line •••), [RuCl(ind){$P(pyr)_3$}$_2$] (dashed line ---).

The cyclic voltammograms of [RuCl(ind)(PPh_3)$_2$] show a high degree of reversibility at different scan rates, as its i_{pc}/i_{pa} values are close to 1 at all scan rates. The $E^{\circ\prime}$ value for the oxidation is –0.023 V (vs. $Cp_2Fe^{0/+}$), and the peak current ratio i_{pc}/i_{pa} is 1.0 at a scan rate of 0.8 V/s. For [RuCl(ind)(PPh_3){$P(pyr)_3$}] and [RuCl(ind){$P(pyr)_3$}$_2$], the $E^{\circ\prime}$ values are significantly higher (+0.34 and +0.71 V, respectively). The oxidation of [RuCl(ind)(PPh_3)-{$P(pyr)_3$}] is still reversible at different scan rates, and the i_{pc}/i_{pa} ratio is 1.0 at 0.8 V/s. However, the oxidation of [RuCl(ind){$P(pyr)_3$}$_2$] only shows some reversibility at high scan rates of 0.8 and 1.6 V/s with low i_{pc}/i_{pa} ratios of 0.7 to 0.8, respectively, which indicate decomposition of the oxidized species. The successive introduction of $P(pyr)_3$ ligands apparently increases the oxidation potential of the respective complexes, which is in line with the higher π-acidic electron demand of that ligand. The presence of two $P(pyr)_3$ ligands in [RuCl(ind){$P(pyr)_3$}$_2$] destabilize the oxidized species [RuCl(ind){$P(pyr)_3$}$_2$]$^+$, as can be seen from the decreased reversibility of the oxidative cyclic voltammogram waves; this suggests that some decomposition occurs after oxidation, possibly by attack of adventitious nucleophiles.

Overall, the combined X-ray diffraction, NMR spectroscopy, and CV data demonstrate that the $P(pyr)_3$ ligand shows π-acidic behavior and is a weaker σ donor than PPh_3. However, as can be seen from the comparable bond lengths and angles for both ligands around the ruthenium center, the $P(pyr)_3$ ligand has steric properties similar to those of PPh_3, despite its profound impact on the electron density at the metal center. Consequently, $P(pyr)_3$ can be utilized in the synthesis of complexes with decreased electron density at the metal center but with steric properties similar to those of their respective PPh_3 derivatives.

Catalytic Applications

We then investigated the ability of the new complexes to activate propargylic alcohols catalytically[29] and chose the etherification of propargylic alcohols **5** as test reactions (Table 3).[15a,15c] The complexes [RuCl(ind)(PPh_3){$P(pyr)_3$}] and [RuCl(ind){$P(pyr)_3$}$_2$] themselves did not show catalytic activity for the reaction. However, after activation through chloride abstraction with Et_3OPF_6, we observed catalytic activity. After some optimization efforts, we found that 1–2 mol-% of activated [RuCl(ind)(PPh_3){$P(pyr)_3$}] catalyzed the etherification of several propargylic alcohols **5** to give the corresponding propargyl ethers **6** in 42 to 27 % isolated yields (toluene solvent, 70 to 95 °C for 16–72 h). The complex [RuCl(ind){$P(pyr)_3$}$_2$] showed no catalytic activity for the etherification reactions in Table 3, even after activation through chloride abstraction. We do not have a satisfactory explanation for the different catalytic activities of the two complexes in the etherification reactions; the alcohol substrates for the etherification reaction possibly deactivate the catalytically active species derived from [RuCl(ind){$P(pyr)_3$}$_2$].

An excess of the alcohol nucleophile over the propargylic alcohol is not required, and the catalyst load of 1–2 mol-% is lower than those of other catalyst systems.[14] Some catalytic systems perform the etherification reactions in Table 3 with the alcohol nucleophile as the solvent.[14] We speculated that the yields could be improved by running the reaction in neat alcohols, and we attempted this for the reactions in Table 3, Entries 3 and 4. In neat *n*-butanol, only trace quantities of the product were observed. In neat benzylic alcohol, conversion to the product was detected by GC, but the starting material **5b** was still present in the reaction mixture. Thus, the reaction is not more efficient with the alcohol nucleophile as the solvent,

Table 3. Isolated yields.

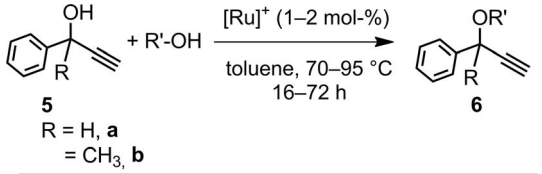

Entry[a]	Substrates	Product	Yield/%
1	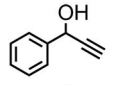 **5a** + 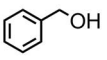	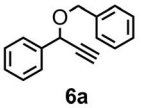 **6a**	38[b]
2	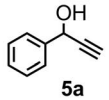 **5a** + 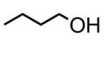	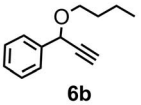 **6b**	37[b]
3	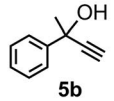 **5b** + 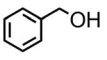	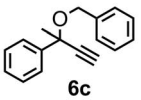 **6c**	42[c]
4	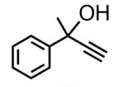 **5b** + 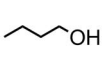	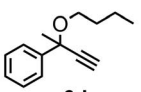 **6d**	41[d]
5	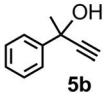 **5b** + 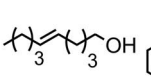	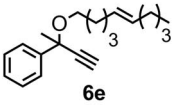 **6e**	27[c]

[a] General conditions: propargylic alcohol (0.7 mmol) and alcohol R′–OH (1 mmol) in toluene (2 mL) catalyzed by activated [RuCl(ind)(PPh_3){$P(pyr)_3$}] (0.007 mmol). The products were isolated chromatographically. [b] 70 °C for 16 h. [c] 85 °C for 18 h. [d] 95 °C for 72 h.

and we tentatively ascribe this to the deactivation of the catalyst by the alcohols.

We then turned our attention to carbon-centered nucleophiles in the form of diketones (Table 4), which have previously been utilized for the substitution of the OH units of propargylic alcohols.[14,29d,29e] When we subjected diketones to the same reaction conditions as those in Table 3, we did not observe the formation of the corresponding substitution products. Instead, we detected xanthenone derivatives **7** in the crude reaction mixtures when cyclohexane-1,3-dione was used as the diketone substrate. Again, after some optimization efforts, we determined that the ruthenium complexes [RuCl(ind)(PPh_3){$P(pyr)_3$}] and [RuCl(ind){$P(pyr)_3$}$_2$], after activation through chloride abstraction, catalyzed the synthesis of the xanthenone derivatives **7a**–**7c** from propargylic alcohols and 2 equiv. of cyclohexane-1,3-dione (80 to 95 °C, 72 h, 67–22 % isolated yields, Table 4). For propargylic alcohol **5b**, the corresponding propargylic acetate **5c** gave higher yields (Table 4, Entry 2). The higher yields might be explained through the fact that the acetate group is a better leaving group than OH. Furthermore, it has been reported that carboxylic acids[30] or trifluoroacetic acid[16j,16k] have beneficial effects on ruthenium-catalyzed isomerization reactions. In line with these reports, the acetate leaving group might convert to acetic acid, which would make the catalyst system more efficient. The identities of the xanthenones **7** were established through X-ray analysis of product **7b** (Figure 5). For **7a**, *E* and *Z* isomers can form during catalysis, and we determined *Z*/*E* ratios of 4.1:1 and 8:1 by ^{1}H NMR spectroscopy for the transformations of **5b** and **5c**, respectively. We tentatively assigned the *Z* configuration to the major isomer of this compound by analogy to a closely related trisubstituted alkene.[31] Product **7c** is known,[32] and was isolated it as the pure *E* isomer, as determined by NMR spectroscopy and comparison of the chemical shifts with the literature values. The high reaction temperatures and somewhat elongated reaction times might promote the formation of the thermodynamically more stable

Table 4. Isolated yields.

Entry	Substrates	Product	
1[a]	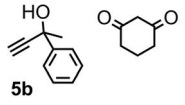 **5b**	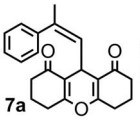 **7a**	22%[b] 34%[c]
2[a]	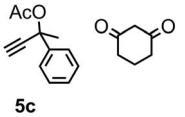 **5c**	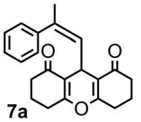 **7a**	46%[b] 67%[c]
3[a]	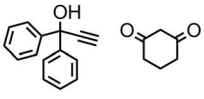 **5d**	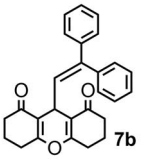 **7b**	69%[c]
4[d]	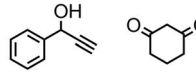 **5a**	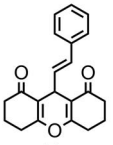 **7c**	29[c]
5[e]	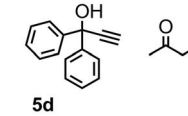 **5d**	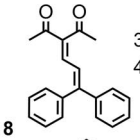 **8**	34%[b] 40%[c]
6[f]	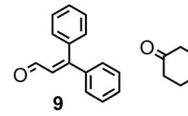 **9**	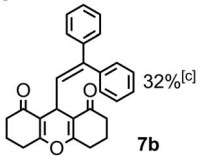 **7b**	32%[c]

[a] Conditions: dione (2.5 equiv.) in $ClCH_2CH_2Cl$ (2 mL) for 72 h at 80–95 °C. The products were isolated chromatographically. [b] Catalyst 1–2 mol-% [Ru(ind){$P(pyr)_3$}$_2$]$^+$. [c] Catalyst 1–2 mol-% [Ru(ind)(PPh_3){$P(pyr)_3$}]$^+$. [d] Conditions: dione (2.5 equiv.) in cyclohexane (2 mL) for 16 h at 90 °C. The products were isolated chromatographically. [e] Conditions: dione (2.5 equiv.) in $Cl_2CH_2CH_2Cl$ (2 mL) for 18–48 h at 85–90 °C. The products were isolated chromatographically. [f] Conditions: dione (2.5 equiv.) in $ClCH_2CH_2Cl$ (2 mL) for 18 h at 85 °C, 4 mol-% catalyst loading. The product was isolated chromatographically.

E isomer. The xanthenones **7a** and **7b** in Table 4 are new, and xanthene derivatives exhibit pharmaceutical activity.[33]

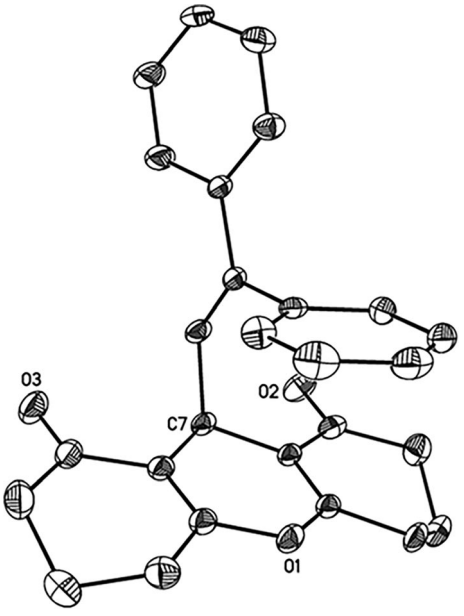

Figure 5. Molecular structure of xanthenone **7b**.

When pentane-2,4-dione was used as the diketone (Table 4, Entry 5), a related reaction occurred in which the diketone condensed with the rearranged propargylic alcohol to give the known conjugated allylidene dione **8**, which has previously been synthesized by utilizing catalytic *p*-toluenesulfonic acid under reflux conditions.[34]

In contrast to the etherification reactions in Table 3, it seemed that activated [RuCl(ind)(PPh_3){P(pyr)$_3$}] and [RuCl(ind)-{P(pyr)$_3$}$_2$] gave comparable yields with diketones.

Although the exact mechanism of the reactions is still to be investigated, the reactions can be viewed as tandem isomerization–condensation sequences (Scheme 2).[35,36] Propargylic alcohols undergo acid-catalyzed Meyer–Schuster rearrangements to their corresponding aldehydes **9** (Scheme 2).[14,37] The aldehydes formed from the propargylic alcohols in Table 4 can then undergo double aldol condensations with the enol tautomers of the diones followed by a hemiacetal formation/dehydration sequence, as suggested by others.[35,36] Indeed, when 3,3-diphenylacrylaldehyde (**9**) was utilized in the reaction with cyclohexane-1,3-dione, **7b** was isolated in a somewhat lower yield of 32 % (Table 4, Entry 6), which suggests that the aldehyde might be an intermediate for the reaction.

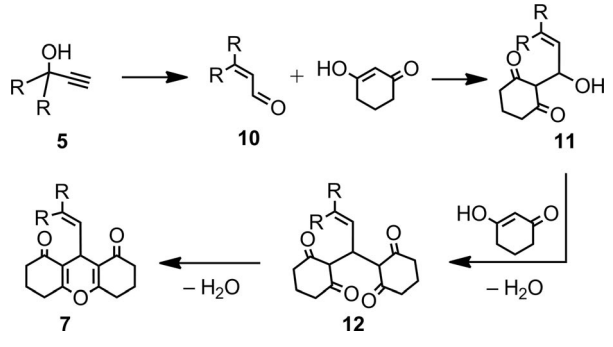

Scheme 2. Tandem isomerization–condensation sequence to give xanthenones **7**.

In principle, the formation of xanthenones from aldehydes and diketones is known and has been achieved with Brønsted[38] or Lewis acid catalysts,[35,39] catalyst-free,[36] or catalyzed by iodine.[40] However, to the best of our knowledge, the chemistry shown in Table 4 and Scheme 2 represents the first examples of the ruthenium-catalyzed conversion of propargylic alcohols (not aldehydes) to xanthenones and the first ruthenium-catalyzed version of the reaction. A gold-catalyzed conversion of propargylic alcohols to xanthenones has been described previously.[41] Further investigations into the mechanism are underway.

Conclusions

The synthesis of the first tris(*N*-pyrrolyl)phosphine indenyl ruthenium complexes [RuCl(ind)(PPh_3){P(pyr)$_3$}] and [RuCl(ind)-{P(pyr)$_3$}$_2$] is described. As determined through X-ray analysis and cyclic voltammetry, the P(pyr)$_3$ ligand is more π-acidic and less σ-donating than PPh_3. However, the steric properties of both ligands in the solid state are comparable, as can be seen from the bond lengths and angles associated with the ruthenium centers derived from X-ray data. After chloride abstraction, the new complexes are catalytically active in the etherification of propargylic alcohols and in a tandem isomerization–condensation sequence to give xanthenones.

Experimental Section

General: All reactions were performed under an inert N_2 atmosphere by using standard Schlenk techniques. All chemicals were used as supplied from Sigma–Aldrich unless otherwise noted. The complex [RuCl(ind)(PPh_3)$_2$] was synthesized by following the literature procedure.[18] THF was distilled from Na/benzophenone under N_2. Ethyl acetate, hexane, toluene, CH_2Cl_2, and $ClCH_2CH_2Cl$ were used as received. Pyrrole was vacuum-distilled from $CaCl_2$ before use. All propargylic alcohols, alcohols, and ketones were obtained and used as provided from Sigma–Aldrich. 1-Phenyl-2-propyn-1-ol and propargyl acetate (**5c**) were synthesized according to literature procedures.[42,43]

The NMR spectra for characterization were collected at room temperature with a Varian Unity 300 MHz or Bruker Avance 300 MHz instrument; all chemical shifts (δ) are reported in ppm and are referenced to a residual solvent signal. The IR spectra were recorded with a Thermo Nicolet 360 FTIR spectrometer. The FAB and exact mass data were collected with a JEOL MStation (JMS-700) mass spectrometer. Melting points were determined with a Thomas Hoover uni-melt capillary melting point apparatus. Elemental analyses were performed by Atlantic Microlab Inc., Norcross, GA, USA.

[RuCl(ind)(PPh_3){P(pyr)$_3$}]: A Schlenk flask containing [RuCl(ind)(PPh_3)$_2$] (0.658 g, 0.848 mmol), P(pyr)$_3$ (0.214 g, 0.932 mmol), and THF (8 mL) was heated gently under reflux for 4 h under nitrogen. The solvent was removed in vacuo. The complex was isolated as a red solid (0.462 g, 0.622 mmol, 73 %) by column chromatography (silica gel 2 × 15 cm, CH_2Cl_2 as eluent); m.p. 120–122 °C (dec.). ^{1}H NMR (300 MHz, $CDCl_3$): δ = 7.51–7.45 (m, 6 H, arom.), 7.33–7.13 (m, 13 H, arom.), 6.14 (br s, 6 H), 6.03 (br s, 6

H), 4.86 (s, 1 H, ind), 4.75 (s, 1 H, ind), 4.54 (s, 1 H, ind) ppm. $^{13}C\{^1H\}$ NMR (75 MHz, $CDCl_3$): δ = 136.9 (d, $J_{C,P}$ = 42.6 Hz), 133.5 (d, $J_{C,P}$ = 10 Hz), 129.8 (s), 129.6 (s), 129.5 (s), 128.2 (d, $J_{C,P}$ = 9.5 Hz), 124.9 (s), 124.4 (s), 124.2 (d, $J_{C,P}$ = 6 Hz), 114.8 (s), 114.7 (s), 111.2 (d, $J_{C,P}$ = 6.5 Hz), 93.9 (s), 70.5 (d, $J_{C,P}$ = 7.5 Hz), 68.3 (d, $J_{C,P}$ = 6.0 Hz) ppm. $^{31}P\{^1H\}$ NMR (121 MHz, $CDCl_3$): δ = 122.81 (d, $J_{P,P}$ = 144 Hz), 40.37 (d, $J_{P,P}$ = 144 Hz) ppm. IR (neat, solid): $\tilde{\nu}$ = 3133 (w), 3052 (w), 2962 (w), 2359 (w), 1454 (m), 1437 (m), 1287 (w), 1178 (s), 1056 (s), 1036 (s), 732 (s), 696 (m), 623 (m) cm^{-1}. HRMS: calcd. for $C_{39}H_{34}N_3P_2{}^{102}Ru$ $[Ru(ind)\{P(pyr)_3\}_2]^+$ 708.1249; found 708.1282. $C_{39}H_{34}ClN_3P_2Ru$ (743.09): calcd. C 63.03, H 4.61; found C 62.77, H 4.59.

$[RuCl(ind)\{P(pyr)_3\}_2]$: A Schlenk flask containing $[RuCl(ind)(PPh_3)\{P(pyr)_3\}]$ (0.140 g, 0.188 mmol), $P(pyr)_3$ (0.086 g, 0.380 mmol), and THF (5 mL) was heated gently under reflux for 5 h under nitrogen. The solvent was removed in vacuo. The complex was isolated as an orange-yellow solid (0.083 g, 0.117 mmol, 62 %) by column chromatography (silica gel 2 × 15 cm, CH_2Cl_2 as eluent); m.p. 126–128 °C (dec.). ^1H NMR (300 MHz, $CDCl_3$): δ = 7.19–7.16 (m, 4 H, arom.), 6.40 (d, $J_{H,H}$ = 1.8 Hz, 12 H), 6.17 (d, $J_{H,H}$ = 1.8 Hz, 12 H), 5.21 (br s, 2 H, ind), 4.75 (br s, 1 H, ind) ppm. $^{13}C\{^1H\}$ NMR (75 MHz, $CDCl_3$): δ = 131.1 (s), 124.4 (s), 124.2 (s), 112.9 (s), 112.4 (s), 96.1 (s), 70.8 (s) ppm. $^{31}P\{^1H\}$ NMR (121 MHz, $CDCl_3$): δ = 122.2 (s) ppm. IR (neat, solid): $\tilde{\nu}$ = 3127 (w), 3106 (w), 1453 (m), 1176 (s), 1083 (m), 1055 (s), 1033 (s), 736 (s), 712 (s), 703 (m), 614 (m) cm^{-1}. HRMS: calcd. for $C_{33}H_{31}N_6P_2{}^{102}Ru$ $[Ru(ind)(PPh_3)\{P(pyr)_3\}]^+$ 675.1138; found 675.1140. $C_{33}H_{31}ClN_6P_2Ru$ (710.08): calcd. C 55.82, H 4.40; found C 55.80, H 4.32.

Activation of $[RuCl(ind)(PPh_3)\{P(pyr)_3\}]$ through Chloride Abstraction: $[RuCl(ind)(PPh_3)\{P(pyr)_3\}]$ was placed in a Schlenk tube with triethyloxonium hexafluorophosphate (1 equiv.) and CH_2Cl_2. The mixture was stirred under N_2 for 2–4 h, and the solvent was removed in vacuo to afford the activated catalyst as a dark tan solid.

[2-(Benzyloxy)but-3-yn-2-yl]benzene (Representative Example for the Catalysis Reactions in Table 3): From 2-phenyl-3-butyn-2-ol (**5b,** Table 3, Entry 3). To a small screw-cap vial containing 2-phenyl-3-butyn-2-ol (**5b**, 0.105 g, 0.72 mmol), benzyl alcohol (0.154 g, 1.4 mmol) was added, along with toluene (2 mL). The activated catalyst was added (0.010 g, 0.007 mmol, 1 mol-%), and the mixture was heated at 100 °C for 72 h. The product **6c** was isolated by column chromatography (silica gel, 1.5 × 15 cm, 2:1 hexane/CH_2Cl_2) as a dark yellow oil (0.071 g, 0.30 mmol, 42 %). The spectroscopic data for all products in Table 3 are given in the Supporting Information and matched the literature values.[15c]

(*Z*)-9-(2-Phenylprop-1-en-1-yl)-3,4,5,6,7,9-hexahydro-1*H*-xanthene-1,8(2*H*)-dione (7a): From propargyl alcohol **5b** (Table 4, Entry 1). To a small screw-cap vial containing 2-phenyl-3-butyn-2-ol (**5b**, 0.138 g, 0.943 mmol), 1,3-cyclohexanedione (0.267 g, 2.381 mmol) was added, along with $ClCH_2CH_2Cl$ (2 mL). The activated catalyst was added (0.010 g, 0.012 mmol, 1.3 mol-%), and the mixture was heated at 80 °C for 72 h. The product was isolated by column chromatography (silica gel, 1.5 × 15 cm, 2:5 ethyl acetate/hexane) as an off-white solid (0.066 g, 0.197 mmol, 21 %) as a 4.2:1 *Z*/*E* mixture of isomers, as assessed by NMR spectroscopy. $C_{22}H_{22}O_3$ (334.16): calcd. C 79.02, H 6.63; found C 79.27, H 6.64.

Major *Z* isomer: ^1H NMR (300 MHz, $CDCl_3$): δ = 7.53–7.09 (m, 5 H, Ph), 5.17 (d, $J_{H,H}$ = 9.9 Hz, 1 H), 4.62 (d, $J_{H,H}$ = 9.9 Hz, 1 H), 2.45 (m, 11 H), 1.97 (m, 4 H) ppm. $^{13}C\{^1H\}$ NMR (75 MHz, $CDCl_3$): δ = 196.7 (s), 164.5 (s), 144.1 (s), 136.3 (s), 128.7 (s), 128.1 (s), 126.7 (s), 126.1 (s), 116.1 (s), 37.2 (s), 27.4 (s), 26.2 (s), 20.6 (s), 16.3 (s) ppm.

Minor *E* Isomer: ^1H NMR (300 MHz, $CDCl_3$, partial): δ = 5.56 (d, $J_{H,H}$ = 8.7 Hz), 4.24 (d, $J_{H,H}$ = 8.7 Hz) ppm. $^{13}C\{^1H\}$ NMR (75 MHz, $CDCl_3$): δ = 163.9 (s), 142.6 (s), 138.0 (s), 128.3 (s), 127.9 (s), 127.3 (s), 126.4 (s), 116.5 (s), 42.3 (s), 38.3 (s), 37.1 (s), 27.8 (s), 27.2 (s), 26.3 (s), 21.9 (s), 20.3 (s) ppm.

From propargyl acetate **5c** (Table 4, Entry 2). To a small screw-cap vial containing 2-phenyl-3-butyn-2-acetate (**5c**, 0.175 g, 0.934 mmol), 1,3-cyclohexanedione (0.265 g, 2.36 mmol) was added, along with $ClCH_2CH_2Cl$ (2 mL). The activated catalyst was added (0.010 g, 0.012 mmol, 1.3 mol-%), and the mixture was heated at 80 °C for 72 h. The product was isolated by column chromatography (silica gel, 1.5 × 15 cm, 2:5 ethyl acetate/hexane) as an off-white solid (0.145 g, 0.435 mmol, 46 %) as an 8:1 mixture of *Z*/*E* isomers, as assessed by NMR spectroscopy. The spectroscopic data matched those reported above.

9-(2,2-Diphenylvinyl)-3,4,5,6,7,9-hexahydro-1*H*-xanthene-1,8(2*H*)-dione (7b): To a small screw-cap vial containing 1,1-diphenylprop-2-yn-1-ol (**5d**, 0.110 g, 0.528 mmol), 1,3-cyclohexanedione (0.212 g, 1.35 mmol) was added, along with $ClCH_2CH_2Cl$ (2 mL). The activated catalyst was added (0.010 g, 0.014 mmol, 2.2 mol-%), and the mixture was heated at 85 °C for 72 h. The product was isolated by column chromatography (silica gel, 1.5 × 15 cm, 2:5 ethyl acetate/hexane) as an off-white solid (0.144 g, 0.363 mmol, 69 %). ^1H NMR (300 MHz, $CDCl_3$): δ = 7.32–7.21 (m, 3 H, Ph), 7.06–7.04 (m, 2 H, Ph), 6.08 (d, $J_{H,H}$ = 9 Hz, 1 H), 4.32 (d, $J_{H,H}$ = 9 Hz, 1 H), 2.23 (m, 8 H), 1.82 (m, 4 H) ppm. $^{13}C\{^1H\}$ NMR (75 MHz, $CDCl_3$): δ = 196.6 (s), 164.3 (s), 143.4 (s), 142.1 (s), 139.9 (s), 130.4 (s), 130.3 (s), 127.9 (s), 127.7 (s), 127.4 (s), 127.0 (s), 126.9 (s), 116.1 (s), 36.9 (s), 27.2 (s), 26.7 (s), 20.6 (s) ppm. $C_{27}H_{24}O_3$ (396.48): calcd. C 81.79, H 6.10; found C 81.63, H 6.12.

(*E*)-9-Styryl-3,4,5,6,7,9-hexahydro-1*H*-xanthene-1,8(2*H*)-dione (7c):[32] To a small screw-cap vial containing 1-phenylprop-2-yn-1-ol (**5a**, 0.133 g, 1.01 mol), 1,3-cyclohexanedione (0.292 g, 2.60 mmol) was added, along with cyclohexane (3 mL). The activated catalyst was added (0.016 g, 0.018 mmol, 1.8 mol-%), and the mixture was heated at 90 °C for 16 h. The product **7c** was isolated by column chromatography (silica gel, 1.5 × 15 cm, 2:5 ethyl acetate/hexane) as an off-white solid (0.095 g, 0.296 mmol, 29 %). ^1H NMR (300 MHz, $CDCl_3$): δ = 7.43–7.18 (m, 5 H, Ph), 6.27 (s, 2 H), 4.72 (s, 1 H), 2.52 (m, 8 H), 2.12 (m, 4 H) ppm. $^{13}C\{^1H\}$ NMR (75 MHz, $CDCl_3$): δ = 196.7 (s), 164.8 (s), 137.5 (s), 131.4 (s), 130.2 (s), 128.5 (s), 127.3 (s), 126.6 (s), 115.7 (s), 37.2 (s), 28.2 (s), 27.4 (s), 20.6 (s) ppm.

3-(3,3-Diphenylallylidene)pentane-2,4-dione (8): To a small screw-cap vial containing 1,1-diphenylprop-2-yn-1-ol (**5d**, 0.111 g, 0.532 mmol), 2,4-pentanedione (0.146 g, 1.45 mmol) was added, along with $ClCH_2CH_2Cl$ (2 mL). The catalyst was added (0.010 g, 0.012 mmol, 2.4 mol-%), and the mixture was heated at 85 °C for 16 h. The product was isolated as a tan oil by column chromatography (silica gel, 1.5 × 12 cm, 2:5 ethyl acetate/hexane). The tan oil was dried in vacuo and dissolved in warm hexanes. As the solution cooled, the product formed as an orange-white solid (0.054 g, 0.186 mmol, 34 %). ^1H NMR (300 MHz, $CDCl_3$): δ = 7.53–7.46 (m, 4 H, Ph), 7.41–7.32 (m, 4 H, Ph), 7.32–7.25 (m, 2 H, Ph), 7.19 (d, $J_{H,H}$ = 11.8 Hz, 1 H), 7.07 (d, $J_{H,H}$ = 11.8 Hz, 1 H), 2.46 (s, 3 H, CH_3), 2.20 (s, 3 H, CH_3') ppm. $^{13}C\{^1H\}$ NMR (75 MHz, $CDCl_3$): δ = 203.6 (s), 197.5 (s), 155.5 (s), 141.9 (s), 140.8 (s), 140.3 (s), 138.2 (s), 130.6 (s),129.6 (s), 129.0 (s), 128.7 (s), 128.5 (s), 128.5 (s), 122.2 (s), 31.9 (s), 26.3 (s) ppm. $C_{20}H_{18}O_2$ (290.26): calcd. C 82.73, H 6.25; found C 82.28, H 6.24.

Cyclic Voltammetry: The voltammograms were recorded with a three-electrode BAS electrochemical cell in a Vacuum Atmospheres HE-493 drybox under an atmosphere of argon with samples in 0.1 M

NBu_4PF_6/CH_2Cl_2 at 298 K. A 1.6 mm Pt disk electrode was used as the working electrode, a platinum wire was used as the auxiliary electrode, and a silver wire was used a pseudoreference electrode. The potentials were calibrated against the $Cp^*_2Fe^{0/+}$ (Cp* = pentamethylcyclopentadienyl) couple, which occurs at –0.548 V versus the $Cp_2Fe^{0/+}$ couple for this solvent.[44] The potentials in this paper can be changed to saturated calomel electrode (SCE) reference values by the addition of 0.56 V. The voltammograms were collected at scan rates of 0.05–1.6 V/s with an EG&G PAR 263A potentiostat interfaced to a computer operated with the EG&G PAR Model 270 software.

X-ray Structure Determination for [RuCl(ind)(PPh_3){P(pyr)$_3$}], [RuCl(ind){P(pyr)$_3$}$_2$], and 7b: Crystals of the metal complexes of appropriate dimension were obtained by the slow diffusion of hexanes into a CH_2Cl_2 solution of the compounds, and crystals of **7b** were obtained by layering an ethyl acetate solution of the compound with hexanes. The crystals were mounted on MiTeGen cryoloops in random orientations. Preliminary examination and data collection were performed with a Bruker X8 Kappa Apex II charge-coupled device (CCD) detector system single-crystal X-ray diffractometer equipped with an Oxford Cryostream LT device. All data were collected with graphite-monochromated Mo-K_α radiation (λ = 0.71073 Å) from a fine-focus sealed-tube X-ray source. The preliminary unit-cell constants were determined with a set of 36 narrow-frame scans. Typical data sets consisted of combinations of ω and Φ scan frames with a typical scan width of 0.5° and a counting time of 15 s per frame at a crystal-to-detector distance of 4.0 cm. The collected frames were integrated by using an orientation matrix determined from the narrow-frame scans. The Apex II and SAINT software packages were used for data collection and data integration.[45] The analysis of the integrated data did not show any decay. The final cell constants were determined by global refinement of reflections harvested from the complete data set. The collected data were corrected for systematic errors by SADABS on the basis of the Laue symmetry by using equivalent reflections.[45]

The crystal data and intensity data collection parameters are listed in Table 1. Structure solutions and refinements were performed with the SHELXTL-PLUS software package.[46] The structures were solved by direct methods and refined successfully in the space groups, *Pbca*, $P2_1/c$, and $P\bar{1}$ for [RuCl(ind)(PPh_3){P(pyr)$_3$}], [RuCl(ind){P(pyr)$_3$}$_2$], and **7b**, respectively. Full-matrix least-squares refinements were performed by minimizing $\Sigma w(F_o^2 - F_c^2)^2$. The non-hydrogen atoms were refined anisotropically to convergence. All hydrogen atoms were treated with an appropriate riding model (AFIX m3). The final residual values and structure refinement parameters are listed in Table 1.

CCDC 1053440 (for **7b**), 1053441 (for [RuCl(ind){P(pyr)$_3$}$_2$]), and 1053442 (for [RuCl(ind)(PPh_3){P(pyr)$_3$}]) contain the supplementary crystallographic data for this paper. These data can be obtained free of charge from The Cambridge Crystallographic Data Centre.

Supporting information (see footnote on the first page of this article): experimental details for the known catalysis products in Table 3, ^1H and ^{13}C NMR spectra for the metal complexes RuCl(ind)(PPh_3)[P(pyr)$_3$] and RuCl(ind)[P(pyr)$_3$]$_2$ and all catalysis products.

Acknowledgments

The National Science Foundation (NSF) is thanked for financial support (grant to E. B. B.: CHE-1300818, grant to M. J. S.: CHE-1213680). Further funding from the NSF for the purchase of the NMR spectrometer (CHE-9974801), the ApexII diffractometer (MRI, CHE-0420497), and the mass spectrometer (CHE-9708640) is acknowledged.

Keywords: Phosphane ligands · Ligand effects · Ruthenium · Structure elucidation · Homogeneous catalysis · Oxidation

[1] a) I. Dragutan, V. Dragutan, A. Demonceau, *Molecules* **2015**, *20*, 17244–17274; b) P. Kumar, R. Kumar Gupta, D. Shankar Pandey, *Chem. Soc. Rev.* **2014**, *43*, 707–733; c) C. Bonaccorsi, A. Mezzetti, *Curr. Org. Chem.* **2006**, *10*, 225–240; d) K. Grela, A. Michrowska, M. Bieniek, *Chem. Rec.* **2006**, *6*, 144–156; e) H. Schaffrath, W. Keim, *J. Mol. Catal. A* **2001**, *168*, 9–14.

[2] a) G. C. Vougioukalakis, A. I. Philippopoulos, T. Stergiopoulos, P. Falaras, *Coord. Chem. Rev.* **2011**, *255*, 2602–2621; b) S. Fantacci, F. De Angelis, *Coord. Chem. Rev.* **2011**, *255*, 2704–2726; c) K. Heinze, K. Hempel, A. Breivogel, *Z. Anorg. Allg. Chem.* **2009**, *635*, 2541–2549.

[3] Representative examples: a) R. F. S. Lee, S. Escrig, M. Croisier, S. Clerc-Rosset, G. W. Knott, A. Meibom, C. A. Davey, K. Johnsson, P. J. Dyson, *Chem. Commun.* **2015**, *51*, 16486–16489; b) R. Trondl, P. Heffeter, C. R. Kowol, M. A. Jakupec, W. Berger, B. K. Keppler, *Chem. Sci.* **2014**, *5*, 2925–2932; c) N. A. Vyas, S. S. Bhat, A. S. Kumbhar, U. B. Sonawane, V. Jani, R. R. Joshi, S. N. Ramteke, P. P. Kulkarni, B. Joshi, *Eur. J. Med. Chem.* **2014**, *75*, 375–381; d) A. Wragg, M. R. Gill, D. Turton, H. Adams, T. M. Roseveare, C. Smythe, X. Su, J. A. Thomas, *Chem. Eur. J.* **2014**, *20*, 14004–14011; e) E. Reisner, V. B. Arion, B. K. Keppler, A. J. L. Pombeiro, *Inorg. Chim. Acta* **2008**, *361*, 1569–1583.

[4] M. J. Clarke, *Coord. Chem. Rev.* **2003**, *236*, 209–233.

[5] a) R. H. Morris, *Acc. Chem. Res.* **2015**, *48*, 1494–1502; b) L. Delaude, A. Demonceau, *Dalton Trans.* **2012**, *41*, 9257–9268; c) A. Mezzetti, *Dalton Trans.* **2010**, *39*, 7851–7869.

[6] Representative examples: a) B. Yu, Y. Xie, F. B. Hamad, K. Leus, A. A. Lyapkov, K. Van Hecke, F. Verpoort, *New J. Chem.* **2015**, *39*, 1858–1867; b) R. Staehle, L. Tong, L. Wang, L. Duan, A. Fischer, M. S. G. Ahlquist, L. Sun, S. Rau, *Inorg. Chem.* **2014**, *53*, 1307–1319; c) S. Enthaler, R. Jackstell, B. Hagemann, K. Junge, G. Erre, M. Beller, *J. Organomet. Chem.* **2006**, *691*, 4652–4659.

[7] Representative examples: a) T. Glöge, K. Jess, T. Bannenberg, P. G. Jones, N. Langenscheidt-Dabringhausen, A. Salzer, M. Tamm, *Dalton Trans.* **2015**, *44*, 11717–11724; b) B. Kali Dey, J. Dutta, M. G. B. Drew, S. Bhattacharya, *J. Organomet. Chem.* **2014**, *750*, 176–184.

[8] C. A. Fleckenstein, H. Plenio, *Chem. Soc. Rev.* **2010**, *39*, 694–711.

[9] K. G. Moloy, J. L. Petersen, *J. Am. Chem. Soc.* **1995**, *117*, 7696–7710.

[10] See, for example: a) R. Menye-Biyogo, F. Delpech, A. Castel, V. Pimienta, H. Gornitzka, P. Riviére, *Organometallics* **2007**, *26*, 5091–5101; b) I. Angurell, I. Martínez-Ruiz, O. Rossell, M. Seco, P. Gómez-Sal, A. Martín, M. Font-Bardia, X. Solans, *J. Organomet. Chem.* **2007**, *692*, 3882–3891; c) I. Angurell, I. Martínez-Ruiz, O. Rossell, M. Seco, P. Gómez-Salb, A. Martín, *Chem. Commun.* **2004**, 1712–1713; d) K. N. Gavrilov, V. N. Tsarev, S. I. Konkin, S. E. Lyubimov, A. A. Korlyukov, M. Yu. Antipin, V. A. Davankov, *Eur. J. Inorg. Chem.* **2005**, 3311–3319; e) A. D. Burrows, M. F. Mahon, M. T. Palmer, M. Varrone, *Inorg. Chem.* **2002**, *41*, 1695–1697; f) C. E. F. Rickard, W. R. Roper, S. D. Woodgate, L. J. Wright, *J. Organomet. Chem.* **2002**, *643–644*, 168–173; g) R. Jackstell, H. Klein, M. Beller, K.-D. Wiese, D. Röttger, *Eur. J. Org. Chem.* **2001**, 3871–3877.

[11] N. A. Foley, M. Lail, T. B. Gunnoe, T. R. Cundari, P. D. Boyle, J. L. Petersen, *Organometallics* **2007**, *26*, 5507–5516.

[12] a) A. D. Burrows, R. W. Harrington, M. F. Mahon, M. T. Palmer, F. Senia, M. Varrone, *Dalton Trans.* **2003**, 3717–3726; b) A. D. Burrows, M. F. Mahon, M. Varrone, *Inorg. Chim. Acta* **2003**, *350*, 152–162; c) A. Huang, J. E. Marcone, K. L. Mason, W. J. Marshall, K. G. Moloy, S. Serron, S. P. Nolan, *Organometallics* **1997**, *16*, 3377–3380.

[13] a) S. Costin, N. P. Rath, E. B. Bauer, *Inorg. Chem. Commun.* **2011**, *14*, 478–480; b) F. Delpech, S. Sabo-Etienne, J.-C. Daran, B. Chaudret, K. Hussein, C. J. Marsden, J.-C. Barthelat, *J. Am. Chem. Soc.* **1999**, *121*, 6668–6682; c) V. Rodriguez, B. Donnadieu, S. Sabo-Etienne, B. Chaudret, *Organometallics* **1998**, *17*, 3809–3814; d) C. Li, S. Serron, S. P. Nolan, *Organometallics* **1996**, *15*, 4020–4029.

[14] E. B. Bauer, *Synthesis* **2012**, *44*, 1131–1151.

[15] a) M. J. Queensen, J. M. Rabus, E. B. Bauer, *J. Mol. Catal. A* **2015**, *407*, 221–229; b) M. J. Queensen, N. P. Rath, E. B. Bauer, *Organometallics* **2014**, *33*, 5052–5065; c) D. F. Alkhaleeli, K. J. Baum, J. M. Rabus, E. B. Bauer, *Catal. Commun.* **2014**, *47*, 45–48; d) A. K. Widaman, N. P. Rath, E. B. Bauer, *New J. Chem.* **2011**, *35*, 2427–2434; e) S. Costin, A. K. Widaman, N. P. Rath, E. B. Bauer, *Eur. J. Inorg. Chem.* **2011**, 1269–1282; f) S. Costin, N. P. Rath, E. B. Bauer, *Tetrahedron Lett.* **2009**, *50*, 5485–5488; g) S. Costin, S. L. Sedinkin, E. B. Bauer, *Tetrahedron Lett.* **2009**, *50*, 922–925; h) S. Costin, N. P. Rath, E. B. Bauer, *Adv. Synth. Catal.* **2008**, *350*, 2414–2424.

[16] For representative examples of ruthenium-catalyzed transformations of propargylic alcohols, see: a) J. Jeschke, C. Gäbler, M. Korb, T. Rüffer, H. Lang, *Eur. J. Inorg. Chem.* **2015**, 2939–2947; b) Y. Senda, K. Nakajima, Y. Nishibayashi, *Angew. Chem. Int. Ed.* **2015**, *54*, 4060–4064; *Angew. Chem.* **2015**, *127*, 4132; c) C. Schreiner, J. Jeschke, B. Milde, D. Schaarschmidt, H. Lang, *J. Organomet. Chem.* **2015**, *785*, 32–43; d) N. Thies, E. Haak, *Angew. Chem. Int. Ed.* **2015**, *54*, 4097–4101; *Angew. Chem.* **2015**, *127*, 4170; e) G. C. Tsui, K. Villeneuve, E. Carlson, W. Tam, *Organometallics* **2014**, *33*, 3847–3856; f) N. Thies, M. Gerlach, E. Haak, *Eur. J. Org. Chem.* **2013**, 7354–7365; g) N. P. Hiett, J. M. Lynam, C. E. Welby, A. C. Whitwood, *J. Organomet. Chem.* **2011**, *696*, 378–387; h) V. Cadierno, J. Francos, J. Gimeno, *Organometallics* **2011**, *30*, 852–862; i) V. Cadierno, J. Francos, J. Gimeno, *Green Chem.* **2010**, *12*, 135–143; j) V. Cadierno, J. Gimeno, N. Nebra, *Adv. Synth. Catal.* **2007**, *349*, 382–394; k) V. Cadierno, S. E. García-Garrido, J. Gimeno, *Adv. Synth. Catal.* **2006**, *348*, 101–110.

[17] For reviews, see: a) V. Cadierno, J. Gimeno, *Chem. Rev.* **2009**, *109*, 3512–3560; b) C.-M. Che, C.-M. Ho, J. S. Huang, *Coord. Chem. Rev.* **2007**, *251*, 2145–2166; c) R. F. Winter, S. Záliš, *Coord. Chem. Rev.* **2004**, *248*, 1565–1583; d) S. Rigaut, D. Touchard, P. H. Dixneuf, *Coord. Chem. Rev.* **2004**, *248*, 1585–1601; e) V. Cadierno, M. P. Gamasa, J. Gimeno, *Eur. J. Inorg. Chem.* **2001**, 571–591; f) M. I. Bruce, *Chem. Rev.* **1998**, *98*, 2797–2858; g) H. Werner, *Chem. Commun.* **1997**, 903–310.

[18] L. A. Oro, M. A. Ciriano, M. Campo, C. Foces-Foces, F. H. J. Cano, *J. Organomet. Chem.* **1985**, *289*, 117–131.

[19] a) M. Pilar Gamasa, J. Gimeno, C. Gonzalez-Bernardo, B. M. Martín-Vaca, D. Monti, M. Bassetti, *Organometallics* **1996**, *15*, 302–308; b) V. Cadierno, J. Díez, M. Pilar Gamasa, J. Gimeno, E. Lastra, *Coord. Chem. Rev.* **1999**, *193–195*, 147–205.

[20] a) S. Nolan, *Acc. Chem. Res.* **2014**, *47*, 3089–3101; b) C. A. Mebi, R. P. Nair, B. J. Frost, *Organometallics* **2007**, *26*, 429–438; c) K. Bieger, J. Díez, M. Pilar Gamasa, J. Gimeno, M. Pavlišta, Y. Rodríguez-Álvarez, S. García-Granda, R. Santiago-García, *Eur. J. Inorg. Chem.* **2002**, 1647–1656; d) P. Alvarez, J. Gimeno, E. Lastra, S. García-Granda, J. F. Van der Maelen, M. Bassetti, *Organometallics* **2001**, *20*, 3762–3771; e) E. P. Kündig, C. M. Saudan, V. Alezra, F. Viton, G. Bernardinelli, *Angew. Chem. Int. Ed.* **2001**, *40*, 4481–4485; *Angew. Chem.* **2001**, *113*, 4613; f) M. Bassetti, S. Marini, F. Tortorella, V. Cadierno, J. Díez, M. Pilar Gamasa, J. Gimeno, *J. Organomet. Chem.* **2000**, *593–594*, 292–298; g) Y. Yamamoto, H. Kitahara, R. Hattori, K. Itoh, *Organometallics* **1998**, *17*, 1910–1912.

[21] a) M. J. Calhorda, L. F. Veiros, *Dalton Trans.* **2011**, *40*, 11138–11146; b) M. J. Calhorda, C. C. Romão, L. F. Veiros, *Chem. Eur. J.* **2002**, *8*, 868–875; c) L. F. Veiros, *Organometallics* **2000**, *19*, 3127–3136; d) J. M. O'Connor, C. P. Casey, *Chem. Rev.* **1987**, *87*, 307–318; e) J. W. Faller, R. H. Crabtree, A. Habib, *Organometallics* **1985**, *4*, 929–935.

[22] G. L. Gibson, K. M. E. Morrow, R. McDonald, L. Rosenberg, *Inorg. Chim. Acta* **2011**, *369*, 133–139.

[23] E. J. Derrah, J. C. Marlinga, D. Mitra, D. M. Friesen, S. A. Hall, R. McDonald, L. Rosenberg, *Organometallics* **2005**, *24*, 5817–5827.

[24] M. Kamigaito, Y. Watanabe, T. Ando, M. Sawamoto, *J. Am. Chem. Soc.* **2002**, *124*, 9994–9995.

[25] a) J. Lodinský, J. Vinklárek, L. Dostál, Z. Růžičková, J. Honzíček, *RSC Adv.* **2015**, *5*, 27140–27153; b) J. Honzíček, J. Vinklárek, M. Erben, J. Lodinský, L. Dostál, Z. Padělkova, *Organometallics* **2013**, *32*, 3502–3511.

[26] a) R. P. Pinnell, C. A. Megerle, S. L. Manatt, P. A. Kroon, *J. Am. Chem. Soc.* **1973**, *95*, 977–978; b) R. D. Kroshefsky, R. Weiss, J. G. Verkade, *Inorg. Chem.* **1979**, *18*, 469–472; c) A. Suárez, M. A. Méndez-Rojas, A. Pizzano, *Organometallics* **2002**, *21*, 4611–4621; d) S. Jeulin, S. Duprat de Paule, V. Ratovelomanana-Vidal, J.-P. Genêt, N. Champion, P. Dellis, *Angew. Chem. Int. Ed.* **2004**, *43*, 320–325; *Angew. Chem.* **2004**, *116*, 324; e) V. Bilenko, A. Spannenberg, W. Baumann, I. Komarov, A. Börner, *Tetrahedron: Asymmetry* **2006**, *17*, 2082–2087; f) D. J. Adams, J. A. Bennett, D. Duncan, E. G. Hope, J. Hopewell, A. M. Stuart, A. J. West, *Polyhedron* **2007**, *26*, 1505–1513; g) S. Enthaler, G. Erre, K. Junge, K. Schröder, D. Addis, D. Michalik, M. Hapke, D. Redkin, M. Beller, *Eur. J. Org. Chem.* **2008**, 3352–3362; h) G. Erre, K. Junge, S. Enthaler, D. Addis, D. Michalik, A. Spannenberg, M. Beller, *Chem. Asian J.* **2008**, *3*, 887–894; i) P. Shejwalkar, S. L. Sedinkin, E. B. Bauer, *Inorg. Chim. Acta* **2011**, *366*, 209–218.

[27] T. S. Barnard, M. R. Mason, *Organometallics* **2001**, *20*, 206–214.

[28] a) B. Suthar, A. Aldongarov, I. S. Irgibaeva, M. Moazzen, B. T. Donovan-Merkert, J. W. Merkert, T. A. Schmedake, *Polyhedron* **2012**, *31*, 754–758; b) A. P. Shaw, J. R. Norton, D. Buccella, L. A. Sites, S. S. Kleinbach, D. A. Jarem, K. M. Bocage, C. Nataro, *Organometallics* **2009**, *28*, 3804–3814; c) A. R. O'Connor, C. Nataro, A. L. Rheingold, *J. Organomet. Chem.* **2003**, *679*, 72–78.

[29] For general examples and reviews regarding the nucleophilic substitution of propargylic alcohols, see: a) K. Nakajima, M. Shibata, Y. Nishibayashi, *J. Am. Chem. Soc.* **2015**, *137*, 2472–2475; b) D.-Y. Zhang, X.-P. Hu, *Tetrahedron Lett.* **2015**, *56*, 283–295; c) B. Wang, C. Liu, H. Guo, *RSC Adv.* **2014**, *4*, 53216–53219; d) F.-Z. Han, F.-L. Zhu, Y.-H. Wang, Y. Zou, X.-H. Hu, S. Chen, X.-P. Hu, *Org. Lett.* **2014**, *16*, 588–591; e) Y. Nishibayashi, *Synthesis* **2012**, *44*, 489–503; f) R. J. Detz, H. Hiemstra, J. H. van Maarseveen, *Eur. J. Org. Chem.* **2009**, 6263–6276; g) N. Ljungdahl, N. Kann, *Angew. Chem. Int. Ed.* **2009**, *48*, 642–644; *Angew. Chem.* **2009**, *121*, 652.

[30] M. Picquet, C. Bruneau, P. H. Dixneuf, *Chem. Commun.* **1997**, 1201–1202.

[31] A. L. Krasovskiy, S. Haley, K. Voigtritter, B. H. Lipshutz, *Org. Lett.* **2014**, *16*, 4066–4069.

[32] V. R. Narayana, Z. Pudukulathan, R. Varala, *Org. Commun.* **2013**, *6*, 110–119.

[33] G. M. Nazeruddin, A. A. Shaikh, Y. I. Shaikh, *Pharm. Lett.* **2011**, *3*, 193–197.

[34] R. Sanz, D. Miguel, A. Martínez, J. M. Álvarez-Gutiérrez, F. Rodríguez, *Org. Lett.* **2007**, *9*, 727–730.

[35] A. Ilangovan, S. Malayappasamy, S. Muralidharan, S. Maruthamuthu, *Chem. Cent. J.* **2011**, *5*, 81–87.

[36] K. Rohr, R. Mahrwald, *Bioorg. Med. Chem. Lett.* **2009**, *19*, 3949–3951.

[37] V. Cadierno, P. Crochet, S. E. García-Garrido, J. Gimeno, *Dalton Trans.* **2010**, *39*, 4015–4031.

[38] a) A. Pramanik, S. Bhar, *Catal. Commun.* **2012**, *20*, 17–24; b) J. Ma, X. Zhou, X. Zang, C. Wang, Z. Wang, J. Li, Q. Li, *Aust. J. Chem.* **2007**, *60*, 146–148l.

[39] X. Fan, X. Hu, X. Zhang, J. Wang, *Can. J. Chem.* **2005**, *83*, 16–20.

[40] N. Mulakayala, P. V. N. S. Murthy, D. Rambabu, M. Aeluri, R. Adepu, G. R. Krishna, C. Malla Reddy, K. R. S. Prasad, M. Chaitanya, C. S. Kumar, M. V. Basaveswara Rao, M. Pal, *Bioorg. Med. Chem. Lett.* **2012**, *22*, 2186–2191.

[41] A. Arcadi, M. Alfonsi, M. Chiarini, F. Marinelli, *J. Organomet. Chem.* **2009**, *694*, 576–582.

[42] a) F. Pünner, G. Hilt, *Chem. Commun.* **2012**, *48*, 3617–3619; b) B. Sathyamoorthy, A. Axelrod, V. Farwell, *Organometallics* **2010**, *29*, 3431–3441.

[43] R. Riveiros, D. Rodríguez, J. Pérez Sestelo, L. A. Sarandeses, *Org. Lett.* **2006**, *8*, 1403–1406.

[44] F. Barrière, W. E. Geiger, *J. Am. Chem. Soc.* **2006**, *128*, 3980–3989.

[45] Bruker Analytical X-ray, Madison, WI, **2012**.

[46] G. M. Sheldrick, *Acta Crystallogr., Sect. A* **2008**, *64*, 112–122.

Received: November 25, 2015
Published Online: January 29, 2016

